

The β Cep/SPB star 12 Lacertae: extended mode identification and complex seismic modelling

J. Daszyńska-Daszkiewicz^{1*}, W. Szewczuk^{1†} and P. Walczak^{1‡}

¹*Instytut Astronomiczny Uniwersytet Wrocławski, Wrocław, Poland*

ABSTRACT

Results of mode identification and seismic modelling of the β Cep/SPB star 12 Lacertae are presented. Using data on the multi-colour photometry and radial velocity variations, we determine or constrain the mode degree, ℓ , for all pulsational frequencies. Including the effects of rotation, we show that the dominant frequency, ν_1 , is most likely a pure $\ell = 1$ mode and the low frequency, ν_A , is a dipole retrograde mode. We construct a set of seismic models which fit two pulsational frequencies corresponding to the modes $\ell = 0, p_1$ and $\ell = 1, g_1$ and reproduce also the complex amplitude of the bolometric flux variations, f , for both frequencies simultaneously. Some of these seismic models reproduce also the frequency ν_A , as a mode $\ell = 1, g_{13}$ or g_{14} , and its empirical values of f . Moreover, it was possible to find a model fitting the six 12 Lac frequencies (the first five and ν_A), only if the rotational splitting was calculated for a velocity of $V_{\text{rot}} \approx 75$ km/s. In the next step, we check the effects of model atmospheres, opacity data, chemical mixture and opacity enhancement. Our results show that the OP tables are preferred and an increase of opacities in the Z -bump spoils the concordance of the empirical and theoretical values of f .

Key words: stars: early-type – stars: oscillations – stars: rotation – stars: individual: 12 Lac – atomic data: opacities

1 INTRODUCTION

The puzzle about the origin of pulsation instability in the B-type main sequence stars had persisted for many years. The explanation of this phenomenon is only 20 years old (Cox et al. 1992, Kiriakidis et al. 1992, Moskalik & Dziembowski 1992, Dziembowski & Pamyatnykh 1993, Gautschy & Saio 1993) and has been possible after re-computation of the opacity data, which included a huge number of transitions in the heavy element ions (Iglesias et al. 1992, Seaton 1993). These new opacities revealed the metal opacity bump around $2 \cdot 10^5$ K, which is called the Z - or Fe-bump, because transitions within the iron M-shell dominate. Since then, many intriguing results have been obtained for the B-type pulsators, mainly thanks to data from the multi-site photometric and spectroscopic campaigns organized for several of such objects as well as from the space-based missions like MOST (Walker et al. 2003), CoRoT (Baglin et al. 2006) or Kepler (Koch et al. 2010). One of the most important results was the discovery of high-order g-modes in early B-type pulsators in which typically low order p/g modes are observed. These variables were termed the β Cep/SPB stars

or hybrid pulsators and a few of them were detected up to now, e.g., ν Eridani (Handler et al. 2004, Aerts et al. 2004, Jerzykiewicz et al. 2005), 12 Lacertae (Handler et al. 2006; Desmet et al. 2009) or γ Pegasi (Handler 2009, Handler et al. 2009). Since the release of the first revised opacity tables many improvements have been added in computation of these atomic data (Iglesias & Rogers 1996, Seaton 1996, 2005). Moreover, the solar chemical mixture has been re-determined several times (Grevesse & Noels 1993, Grevesse & Sauval 1998, Asplund et al. 2005, 2009). Despite of that, still a common problem is to get the high-order g-modes excited in models with masses larger than about $7 M_{\odot}$.

The hybrid pulsators give challenges as well as possibilities. Excitation of both low order p/g modes and high order g-modes allow potentially to scan almost the whole interior of a star. On the other hand, the problem with instability of high-order g-modes indicates that there is still something we do not understand or cannot adequately take into account in stellar physics. Usually, the opacity data are „blamed” for the inconsistencies and an artificial increase of the opacity coefficient was called, e.g., for the ν Eri star (Pamyatnykh, Handler & Dziembowski 2004).

In this paper we reanalyse the frequency spectrum of the hybrid B-type pulsator 12 Lacertae. In Section 2, we give an overview of the star. Section 3 is devoted to mode identifi-

* E-mail: daszynska@astro.uni.wroc.pl

† E-mail: szewczuk@astro.uni.wroc.pl

‡ E-mail: walczak@astro.uni.wroc.pl

ation, which we made both within the zero-rotation approximation and including some effects of rotation for frequencies which can be mostly affected by it. In Section 4, we present results of seismic modelling which we made in two steps, i.e., 1) fitting frequencies and 2) fitting the nonadiabatic f -parameter. We study the effects of model atmospheres, opacity data, chemical mixture and opacity enhancement. Conclusions are summarised in Section 5.

2 THE VARIABLE STAR: 12 LACERTAE

12 Lacertae (DD Lac, HR 8640, HD 214993) is a well-known pulsating star of B2III spectral type. Studies of the variability of the star have begun in the early twentieth century when Adams (1912) discovered its radial velocity variations. The period of these changes amounted to $P = 0^d.193089$ as determined by Young (1915).

In the following years 12 Lac had been extensively studied by many authors, e.g. Young (1919), Christie (1926). However, the physical interpretation of the radial velocity changes was incorrect; they thought that 12 Lac is a binary system. Stebbins (1917) and Guthnick (1919) reported the light variations with periods of $0^d.193$ and $0^d.1936$, respectively, which agreed well with the spectroscopic value of Young (1915). Fath (1938) explained a shape of the light curve as an interference between two close periods of the order of $0^d.193$. In his further studies, Fath (1947) found three periods; the well-known primary $0^d.19308902$, the secondary $0^d.164850$ and the third $0^d.1316$. However, these periods have not been confirmed by de Jager (1953), who determined the new value of the primary period $0^d.1930883$ and found the secondary $0^d.197367$. In 1956, one of the first worldwide observing campaigns was organized called The International Lacertae weeks (de Jager 1963). The analysis of these observations by Barning (1963) led to a discovery of four different periods; two already known: $0^d.1930883$, $0^d.197358$, and two new ones: $0^d.182127$, $25^d.85$. Jerzykiewicz (1978) chose a more homogeneous sample of yellow passband data from this campaign and detected six periods: $P_1 = 0^d.1930754$, $P_2 = 0^d.19737314$, $P_3 = 0^d.18214713$, $P_4 = 0^d.1874527$, $P_5 = 0^d.0951112$ and $P_6 = 0^d.23582180$.

Sato (1979) examined observational data of 12 Lac to test stability of pulsational periods. Next, secular variations of the period were searched by Ciurla (1987), but no variations larger than 0.08 s per century were found. After the great effort made during The International Lacertae weeks more photometric data were gathered and analysed by Jarzebowski et al. (1979) and Jerzykiewicz et al. (1984). Smith (1980) examined SiIII λ 4567 line profile variations. His findings were generally in agreement with previous results of Jerzykiewicz (1978). The spectroscopic analysis based on high spectral and time resolution observations had been carried out by Mathias et al. (1994). Their frequency analysis revealed a presence of 6 photometric frequencies in the radial velocity curve. Subsequently Dziembowski & Jerzykiewicz (1999) investigated the possibility of existence of the equidistant triplet, ν_1, ν_4, ν_3 (corresponding to periods P_1, P_4 and P_3) and performed seismic modelling.

In the years 2003-2004, the two multisite campaigns

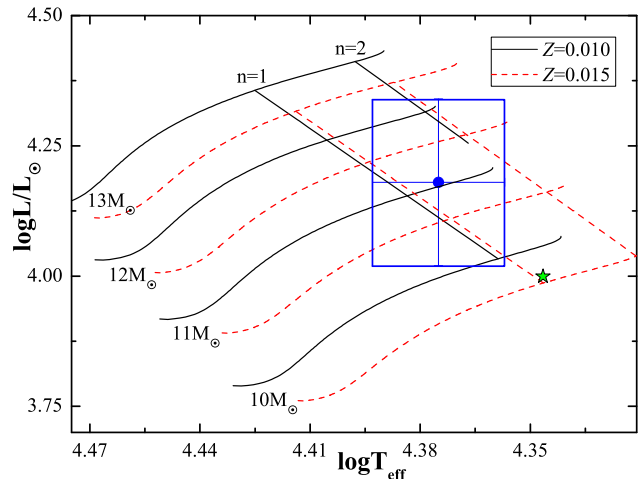


Figure 1. The HR diagram with a position of the observational error box of 12 Lac as determined by Handler et al. (2006). The evolutionary tracks were computed for two values of metallicity, $Z = 0.010, 0.015$, the hydrogen abundance of $X = 0.7$, initial rotational velocity of $V_{\text{rot}} = 50$ km/s, no overshooting from the convective core and the OPAL tables. Lines labeled as $n = 1, n = 2$ and an asterisk will be discussed later in the text.

for 12 Lac were organized. Handler et al. (2006) reported results on the photometric campaign; they confirmed five from six already known frequencies and added six new independent modes, including the low frequency typical for Slowly Pulsating B-type stars (SPB). The frequency values determined from these data are: $\nu_1=5.179034$, $\nu_2=5.066346$, $\nu_3=5.490167$, $\nu_4=5.334357$, $\nu_5=4.24062$, $\nu_6=7.40705$, $\nu_7=5.30912$, $\nu_8=5.2162$, $\nu_9=6.7023$, $\nu_{10}=5.8341$ and $\nu_A=0.35529$ c/d. Based on the colour photometry Handler et al. (2006) provided the spherical degrees ℓ for the five strongest frequency peaks and constraints on ℓ for the low-amplitude frequencies. Then, Desmet et al. (2009) presented results on the spectroscopic campaign. They confirmed 10 independent frequencies discovered from photometry. The important result was that in their spectroscopy the SPB-type frequency has been also detected. Thus, 12 Lac is another known hybrid pulsator in which the β Cep and SPB type modes are excited simultaneously. From spectroscopy, Desmet et al. (2009) arrived at a unique identification of the mode degrees, ℓ , and azimuthal orders, m , for four pulsational frequencies.

Dziembowski & Pamyatnykh (2008), based on results from the 2003 world-wide campaign, made seismic modelling of 12 Lac and showed that the rotation rate increases significantly towards the star centre. They addressed also a problem with excitation of low frequency mode ν_A .

In Fig. 1, we show the observational error box of 12 Lac in the HR diagram. The star is in an advanced phase of the core hydrogen burning. We adopted the effective temperature, $\log T_{\text{eff}} = 4.375 \pm 0.018$ and luminosity, $\log L/L_{\odot} = 4.18 \pm 0.16$ from Handler et al. (2006). In the literature various determinations of metallicity are given. Niemczura & Daszyńska-Daszkiewicz (2005) obtained $[m/H] \approx -0.2 \pm 0.1$ from the ultraviolet IUE spectra, which corresponds to $Z \approx 0.012 \pm 0.003$, whereas Morel et al. (2006) derived $Z = 0.0089 \pm 0.0018$ from the high resolution optical spectra. Therefore, we show evolutionary tracks for two values

of metallicity: $Z = 0.015$ and $Z = 0.010$. Computations were performed using the Warsaw-New Jersey evolutionary code (Pamyatnykh et al. 1998), with the OPAL equation of state (Rogers & Nayfonov 2002), the OPAL opacity tables (Iglesias & Rogers 1996) and the latest heavy element mixture by Asplund et al. (2009), hereafter AGSS09. For lower temperatures, the opacity data were supplemented with the Ferguson tables (Ferguson et al. 2005; Serenelli et al. 2009). We assumed the hydrogen abundance of $X = 0.7$, initial rotational velocity of $V_{\text{rot}} = 50$ km/s and no overshooting from the convective core. Rotational velocity was chosen of the same magnitude as in Desmet et al. (2009) who derived $V_{\text{rot}} \sin i = 36 \pm 2$ km/s and $V_{\text{rot}} = 49 \pm 3$ km/s. It means that 12 Lac rotates at a speed of about 10% of its break-up velocity ($V_{\text{rot}}^{\text{crit}} \approx \sqrt{\frac{GM}{R}} \approx 480$ km/s).

3 MODE IDENTIFICATION

To identify pulsational modes detected in 12 Lac, we will use the most popular observables, i.e., the amplitudes and phases of the photometric and radial velocity variations. Here, we rely on the Strömgren *uvy* photometry (Handler et al. 2006) and the radial velocity changes (Desmet et al. 2009) determined as the first moment of the SiIII 4552.6Å line. We performed mode identification in two steps. Firstly, we determined the degree ℓ ignoring all effects of rotation on pulsation. This is a commonly used approach and in the case of 12 Lac, which rotates at a speed of about 50 km/s, seems to be justified for the most frequencies. However, this value of rotation can already couple pulsational modes and affects properties of slow modes such as the frequency ν_A detected in 12 Lac. Therefore, in the second step, we checked whether the dominant frequency, ν_1 , can be a rotational coupled mode and apply traditional approximation to identify the angular numbers of the low frequency, ν_A .

3.1 The zero-rotation approximation

If all effects of rotation on stellar pulsation are neglected then identification of the mode degree, ℓ , from photometric amplitudes and phases are independent of the inclination angle, i , intrinsic mode amplitude, ε , and azimuthal order, m . This is also a disadvantage of disregarding rotation because the full geometry of mode cannot be determined. Within the zero-rotation approximation, the complex amplitude of the light variation in the x passband in the framework of linear theory can be written as (e.g., Daszyńska-Daszkiewicz et al. 2002)

$$\mathcal{A}^x(i) = -1.086\varepsilon Y_\ell^m(i, 0) b_\ell^x (D_{1,\ell}^x + D_{2,\ell} + D_{3,\ell}^x), \quad (1)$$

where Y_ℓ^m is the spherical harmonic, b_ℓ^x is disc averaging factor, and $D_{1,\ell}^x$, $D_{2,\ell}$ and $D_{3,\ell}^x$ are the temperature, geometrical and pressure effects, respectively. Expressions for these quantities can be found in Daszyńska-Daszkiewicz et al. (2002).

The radial velocity variations due to pulsations are defined as the first moment of the well isolated spectral line and the formulae is given in Dziembowski (1977).

To compute the theoretical values of the photometric amplitudes and phases two inputs are needed. The first one

comes from models of stellar atmospheres and these are pass-band flux derivatives over effective temperature and gravity as well as limb darkening, included in the terms $D_{1,\ell}^x$ and $D_{3,\ell}^x$, respectively. Here, we rely on two grids of stellar atmosphere models: LTE (Kurucz 2004) and non-LTE (Lanz & Hubeny 2007) and consider different values of the atmospheric metallicity, $[m/H]$, and the microturbulent velocity, ξ_t . The second input is connected with pulsational properties and this is the so-called nonadiabatic complex parameter f describing a ratio of the amplitude of the radiative flux perturbation to the radial displacement at the photosphere level (e.g. Daszyńska-Daszkiewicz, Dziembowski, Pamyatnykh 2003). The f -parameter is incorporated in the temperature term, $D_{1,\ell}^x$.

A comprehensive overview of possible sources of uncertainties in the theoretical values of the photometric amplitudes and phases of early B-type pulsators has been studied in details by Daszyńska-Daszkiewicz & Szewczuk (2011).

The value of f for a given mode can be either obtained from the linear nonadiabatic computations of stellar pulsations (Cugier, Dziembowski, Pamyatnykh 1994) or determined from observations (Daszyńska-Daszkiewicz et al. 2003, 2005). Here, we applied the two approaches.

To identify the degree ℓ of pulsational modes of 12 Lac using the theoretical f -parameter, we compared the theoretical and observational values of the photometric amplitude ratios and phase differences in various pairs of passbands. To this aim, we considered models from the error box corresponding to masses from 10 to 12 M_\odot and used the nonadiabatic pulsational code of Dziembowski (1977). To check how our identification of ℓ is robust we considered two values of metallicity, $Z = 0.015$ and 0.010, two chemical mixtures, AGSS09 and GN93 (Grevesse & Noels (1993)), two sources of the opacity tables, OPAL (Iglesias & Rogers 1996) and OP (Seaton 2005), and two sets of stellar model atmospheres, LTE and non-LTE. The hydrogen abundance was fixed at $X = 0.7$ and no overshooting from the convective core was allowed. We considered the values of ℓ from 0 up to 6 and the frequency range appropriate to the observational values.

Using the theoretical values of f , we arrived at the following identification. The dominant mode ν_1 as well as ν_2 are certainly dipoles ($\ell = 1$). Identification of ℓ for ν_3 and ν_5 is also unique; they are quadruple modes ($\ell = 2$). There is also no doubt about identification of ℓ for ν_4 ; certainly this is a radial mode ($\ell = 0$). Identification of ℓ for the remaining frequencies is ambiguous: ν_6 is most likely a dipole, but it may be also $\ell = 2$ or 3; ν_7 can be $\ell = 1, 2, 3, 5$; for ν_8 we were not able to associate any values of ℓ ; ν_9 is either $\ell = 3$ or 1 and ν_{10} can be $\ell = 1$ or 2 or 3. Finally for the SPB like mode, ν_A , we got $\ell = 1$ or 6, but because of the strong averaging effects which increase with the harmonic degree, the $\ell = 6$ identification is much less probable. These identifications are independent of the metallicity, opacity data, mixture and atmosphere models. An influence of the different stellar parameters (within the error box) is also negligible.

In the second approach the mode degree ℓ is determined simultaneously with the empirical values of f by fitting the theoretical values of the photometric amplitudes and phases to the observational counterparts (Daszyńska-Daszkiewicz et al. 2003, 2005). To this end we considered stellar parameters from the center and edges of the error box. We checked

Table 1. The most probable identification of ℓ for the 12 Lac frequencies obtained from two methods described in the text. In the last column, we put the values of m determined by Desmet et al. (2009).

frequency [c/d]	A_V [mmag]	the most probable ℓ		m Desmet2009
		theoret. f	empir. f	
$\nu_1=5.179034$	38.1	1	1	1
$\nu_2=5.066346$	16.0	1	1	0
$\nu_3=5.490167$	11.1	2	2	1
$\nu_4=5.334357$	10.0	0	0	0
$\nu_5=4.24062$	3.6	2	2	0,1,2
$\nu_6=7.40705$	2.0	1,2,3	1,2	–
$\nu_7=5.30912$	2.0	1,2,3,5	–	–
$\nu_8=5.2162$	1.3	?	2	–
$\nu_9=6.7023$	1.3	3,1	3,1	–
$\nu_{10}=5.8341$	1.3	1,2,3	1,2	–
$\nu_A=0.35529$	5.0	1,6	1,4	–

also the effects of adopted model atmospheres, i.e., effects of the microturbulent velocity, ξ_t , metallicity, [m/H], as well as the non-LTE effects. All the above parameters do not change identification of ℓ although a quality of the fit obtained with the LTE and non-LTE models can differ significantly. Usually, with the non-LTE atmospheres we got the better goodness of the fit. From this approach, we found a unique determination of ℓ for the six frequencies. For the first five modes with the largest amplitudes results are consistent with the determinations obtained with the theoretical values of the f -parameter. In the case of some other frequencies we succeed in getting better constraints on ℓ , i.e., ν_6 and ν_{10} can be $\ell = 1$ or 2 and $\ell = 3$ is excluded, ν_8 has been identified uniquely as a quadruple. The degree of ν_7 is indeterminable because this frequency has not been detected in spectroscopy. The slow mode ν_A is now $\ell = 1$ or 4 .

In Table 1, we list frequencies of 12 Lac and the most probable identification of the degree ℓ from the two approaches. The last column contains the values of m as determined by Desmet et al. (2009). As we can see, identifications of ℓ from the two methods are consistent. In the case of ν_A , the common identification is $\ell = 1$ and this is the most likely degree. Moreover, the visibility of modes with $\ell = 4$ and 6 is much lower. Our identifications of ℓ agree with those obtained by Handler et al. (2006).

From the second approach, besides the degree ℓ , we get the empirical value of f , which has a great astroseismic potential, and the intrinsic mode amplitude multiplied by the aspect factor, $\tilde{\varepsilon} = \varepsilon Y(i, 0)$. These quantities will be discussed in subsequent sections.

3.2 Including effects of rotation

Rotation causes that the $2\ell + 1$ degeneracy is lifted what allows to determine the full geometry of pulsational modes, i.e., the spherical harmonic degree, ℓ , and azimuthal order, m . It also complicates mode identification because the photometric amplitude ratios and phase differences become dependent on the inclination angle and rotational velocity.

In the case of low order p- and g-modes, the most important effects of rotation is mode coupling occurring for close frequency modes with the same values of m and ℓ dif-

fering by 2 (Soufi, Goupil & Dziembowski, 1998). The two modes are close if the difference between their frequencies is of the order of the rotational frequency, i.e., $|\nu_1 - \nu_2| \approx \nu_{\text{rot}}$. Then, the complex photometric amplitude due to a pulsational mode coupled by rotation is given as a sum of the photometric amplitudes of modes contributing to the coupling (Daszyńska-Daszkiewicz et al. 2002)

$$\mathbf{A}_\lambda^{\text{coup}}(i) = \sum_k a_k \mathcal{A}_{\lambda,k}(i), \quad (2)$$

where $\mathcal{A}(i)$ is given in Eq. 1. The coefficients a_k results from linear perturbation theory of rotating stars and describe contributions of the ℓ_k -modes to the coupled mode.

According to Desmet et al. (2009), the surface equatorial rotational velocity of 12 Lac amounts to about 50 km/s. Adopting the stellar radius of about $7 R_\odot$ we get a surface rotational frequency of about $\nu_{\text{rot}} = 0.14$ c/d. As has been shown by Daszyńska-Daszkiewicz et al. (2002), already rotation of this order can couple modes.

The dominant mode of 12 Lac, which has been identified as the $\ell = 1$ mode, has the photometric amplitude much higher than the other ones; its value of A_V is about 2.5 larger than for ν_2 . **Because usually, it is the radial mode which dominates, we checked whether ν_1 could be the $\ell = 0$ mode coupled with the $\ell = 2$ mode by rotation.** Pulsational models which satisfy the rotational coupling conditions for the frequency ν_1 can be found in a very wide range of stellar parameters within the 12 Lac error box.

In Fig. 2, we show an example of a mode coupling between the $\ell = 0, p_1$ and $\ell = 2, g_1$ modes with frequencies before the coupling of about 5.17 and 5.15 c/d, respectively. The parameters of the model are: $M = 9.43M_\odot$, $\log T_{\text{eff}} = 4.3411$ and $\log L/L_\odot = 3.975$. The value of $V_{\text{rot}} \sin i = 36$ km/s was kept constant and the values of V_{rot} are indicated at each point. The pure modes with $\ell = 0, 1, 2$ are marked as big dots. The observational position for the frequency ν_1 is shown as an asterisk. As we can see the best agreement is obtained if ν_1 is considered as the pure $\ell = 1$ mode. The same conclusion was reached for other models of 12 Lac and other pairs of modes. Therefore, in our further analysis we assume that ν_1 is the pure $\ell = 1$ mode.

In the case of high-order g-modes, whose frequencies are of the order of the rotational frequency, incorporation of the Coriolis force is crucial. One way to account for these effects of rotation is the so-called traditional approximation (e. g. Lee & Saio 1987, Townsend 2003). In the case of the low frequency of 12 Lac, $\nu_A = 0.35529$ c/d, the spin parameter, $s = 2\nu_{\text{rot}}/\nu$, amounts to 0.8-1.0 depending on the model. At such value of s , the photometric amplitudes and phases can be changed. The effects of rotation on photometric observables for high-order g-modes excited in the SPB star models were studied by Townsend (2003). The formulas for the light and radial velocity variations, we use here, were given by Daszyńska-Daszkiewicz, Dziembowski & Pamyatnykh (2007). The semi-analytical form of the formula for the complex amplitude of the light variations due to pulsations in a high-order g-mode is as follows:

$$\mathbf{A}_\lambda^{\text{trad}}(i) = \sum_j \gamma_{\ell_j} \mathcal{A}_{\lambda,\ell_j}(i), \quad (3)$$

where γ_{ℓ_j} are coefficients of the expansion of the Hough function into the series of the Legendre functions (see Daszyńska-

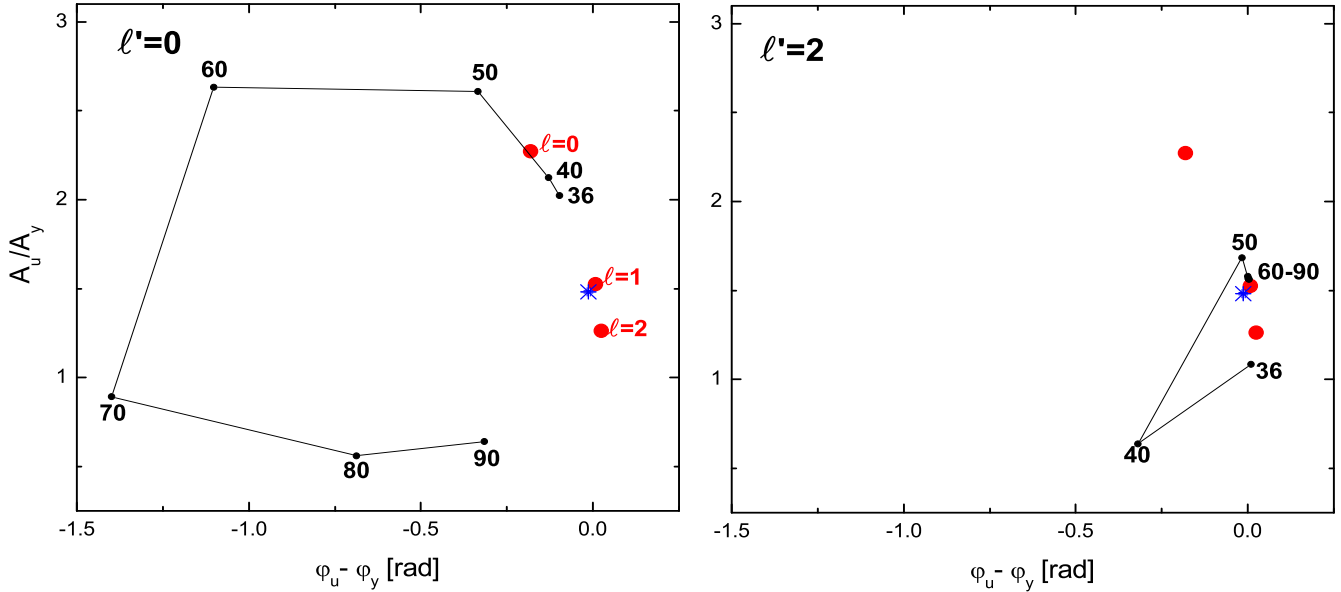


Figure 2. The diagnostic diagrams with Strömrgren passbands u and y , showing positions for coupled $\ell = 0, p_1$ and $\ell = 2, g_1$ modes excited in the model with $M = 9.43M_{\odot}$, $\log T_{\text{eff}} = 4.3411$ and $\log L/L_{\odot} = 3.975$. Big dots indicate positions of the pure modes with $\ell = 0, 1, 2$. The numbers at small dots are the values of the rotational velocity in km/s. The values of the inclination angle result from the condition $V_{\text{rot}} \sin i = 36$ km/s. An asterisk denotes an observational position of ν_1 with errors.

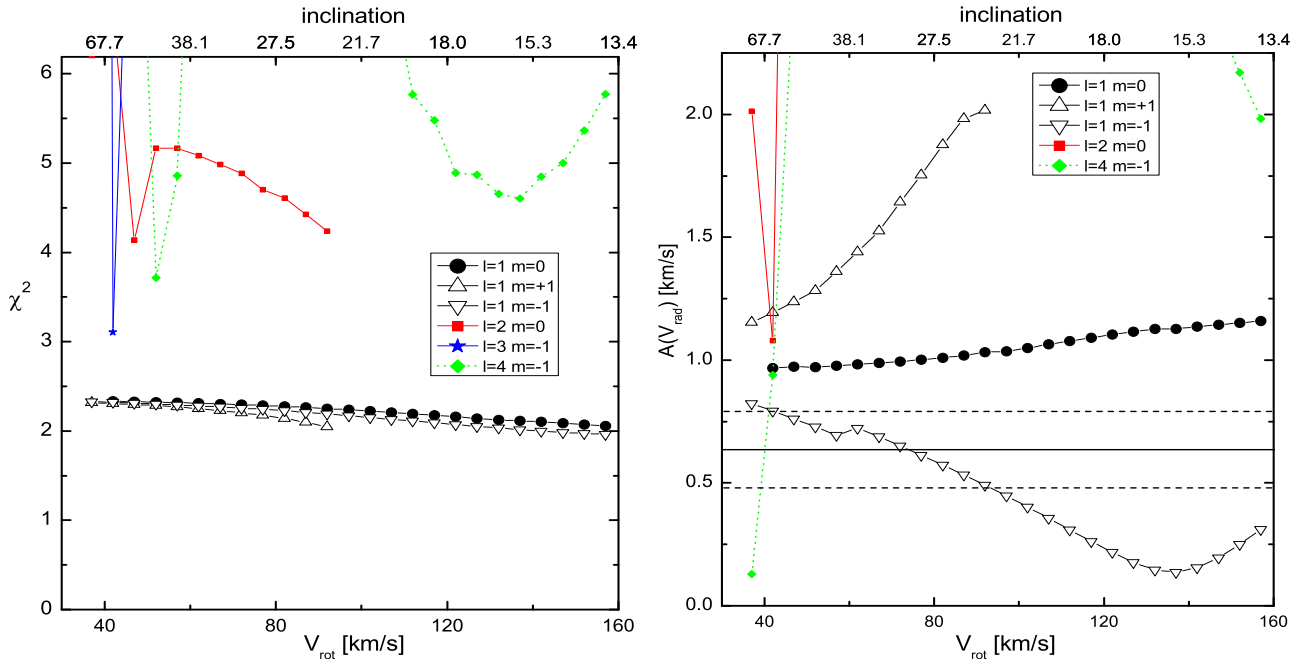


Figure 3. Left panel: the values of χ^2 for the ν_A frequency as a function of the rotational velocity. Only unstable modes in the model with $M = 9.91M_{\odot}$, $\log T_{\text{eff}} = 4.3546$ and $\log L/L_{\odot} = 4.039$ were included. The corresponding values of the inclination angle result from a condition $V_{\text{rot}} \sin i = 36$ km/s and are indicated at the top X axis. Right panel: the resulting amplitudes of the radial velocity variations calculated for the optimal values of ε . The observational range of $A(V_{\text{rad}})$ is marked as horizontal lines.

Daszkiewicz, Dziembowski & Pamyatnykh, 2007) and $\mathcal{A}(i)$ is given in Eq. 1.

In order to determine the angular numbers of ν_A , we apply the same discriminant, χ^2 , as proposed by Daszyńska-Daszkiewicz, Dziembowski & Pamyatnykh (2008). The χ^2

discriminant includes the best value of the intrinsic mode amplitude, ε , to fit photometric amplitudes and phases in all passbands simultaneously. The value of χ^2 is a function of both the inclination angle and rotational velocity.

In the left panel of Fig. 3, we plot the dependence of

χ^2 on the rotational velocity for unstable modes with frequencies close to ν_A . Again the value of $V_{\text{rot}} \sin i = 36$ km/s was kept constant. We show an example for model with the following parameters: $M = 9.91 M_{\odot}$, $\log T_{\text{eff}} = 4.3546$ and $\log L/L_{\odot} = 4.039$. Only modes which give $\chi^2 < 6$ were shown. As we can see, all dipole modes are acceptable. For a possible discrimination of the azimuthal order, m , in the right panel of Fig. 3, we plotted the amplitude of the radial velocity variations obtained for the best value of ε as a function of V_{rot} . The horizontal lines mark the observed value of $A(V_{\text{rad}})$ with errors. We can see that only the retrograde mode ($\ell = 1$, $m = -1$) has the radial velocity amplitude within the observational range. This identification does not change if other models of 12 Lac are considered. Thus, we assume that ν_A is a dipole retrograde mode.

3.3 Radial orders of pulsational modes

Our assignment of the radial order, n , has been done within the zero-rotation approximation. For non-axisymmetric frequencies with the identified azimuthal order, m , we estimated the centroid frequency, $\nu_{n\ell}$, from the following equation

$$\nu_{n\ell m} = \nu_{n\ell} + (1 - C_{n\ell})m\nu_{\text{rot}}, \quad (4)$$

where $C_{n,\ell}$ is the Ledoux constant and ν_{rot} is the rotational frequency.

In the HR diagram (Fig. 1), we plotted the lines of constant period $P = 0.18746$ d, corresponding to the radial mode ν_4 , assuming that ν_4 is the fundamental ($n = 1$) or first overtone mode ($n = 2$). Two values of metallicity, $Z = 0.01$ and 0.015 , were considered. Both lines are within the error box, but the $n = 2$ line is cut near the middle, for the lower metallicity models. It is caused by a lack of the main sequence models reproducing ν_4 with masses lower than about $11 M_{\odot}$ for $Z = 0.01$.

In order to identify the radial order, n , of ν_4 , we compared the empirical and theoretical values of the nonadiabatic f -parameter (Daszyńska-Daszkiewicz, Dziembowski & Pamyatnykh, 2003, 2005). We chose models which are located on lines of constant period and are inside the observational error box of 12 Lac. For these models, we computed the theoretical values of f for the frequency ν_4 and compare them with the empirical counterparts. The results are presented in Fig. 4, where the real part of the f -parameter, f_{R} , is plotted against its imaginary part, f_{I} . The empirical values are marked as a box and the theoretical ones as lines with symbols corresponding to the three values of metallicity: $Z = 0.010, 0.013, 0.015$. All models were computed with the OP opacities and no overshooting from the convective core. In the upper panel of Fig. 4, we assumed that ν_4 is the fundamental mode, while in the bottom panel - the first overtone.

As we can see, the agreement is achieved if ν_4 is the radial fundamental mode. Moreover, all these models are unstable, while in the case of the first overtone, only models to the right of the thin, black line labeled as $\eta = 0.0$ are unstable. We need quite high metallicity and large masses to make ν_4 unstable as a first overtone. With the OPAL data, identification of n is not so unambiguous but a requirement of instability and lower values of Z make the first overtone

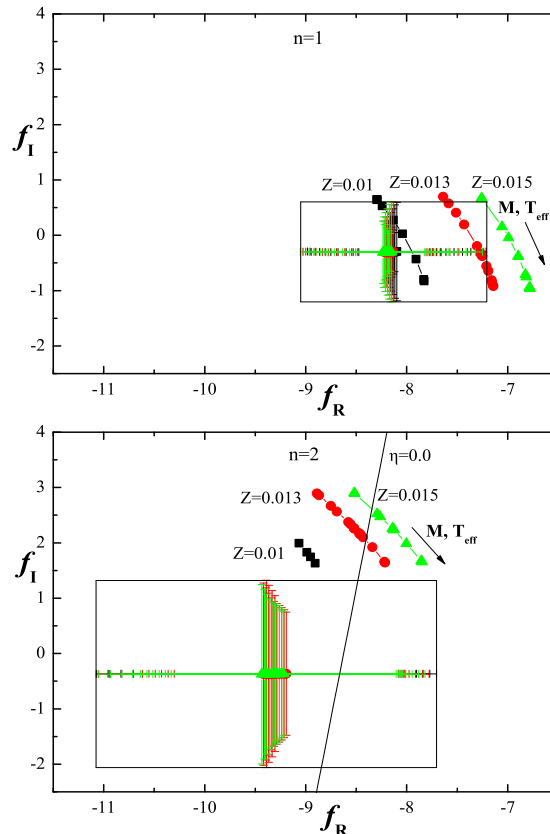


Figure 4. Comparison of the empirical (boxes) and theoretical (lines with symbols) values of f for the radial mode, ν_4 , on the complex plane. The upper and bottom panels correspond to the hypothesis of the fundamental and first overtone radial mode, respectively. The theoretical values of the f -parameter were calculated with the OP tables for three values of metallicity, $Z = 0.01, 0.015$ and 0.02 . All models reproduce the frequency ν_4 and are inside the error box of 12 Lac. The thin, black line in the bottom panel indicates the instability border. Models to the right of this line are unstable. In the upper panel, all models are unstable. The arrows indicate the increasing masses and effective temperatures.

also much less likely. **The effect of the overshooting parameter, α_{ov} , on identification of n is completely negligible.** Thus, we adopted that ν_4 is the radial fundamental mode in our further analysis. Our identification of n for the frequency ν_4 confirms that of Dziembowski & Pamyatnykh (2008)

Following Desmet et al. (2009), we assumed that the dipole mode ν_2 is axisymmetric ($m = 0$). A survey of pulsational models with different masses, M , metallicities, Z , and core overshooting parameters, α_{ov} , showed, that if ν_4 is the radial fundamental mode, then ν_2 can be only the g_1 mode. To account for the rotational splitting of ν_1 and ν_2 , which belong to the $\ell = 1$, g_1 triplet, Dziembowski & Pamyatnykh (2008) suggested a nonuniform rotation with an increase of its rate between the envelope and core. Therefore, we considered rotational splitting according to the two values of the rotational velocity: 50 and 80 km/s. The values of the Ledoux constant were appropriate for models of 12 Lac. Identification of n for the first five modes is consistent for

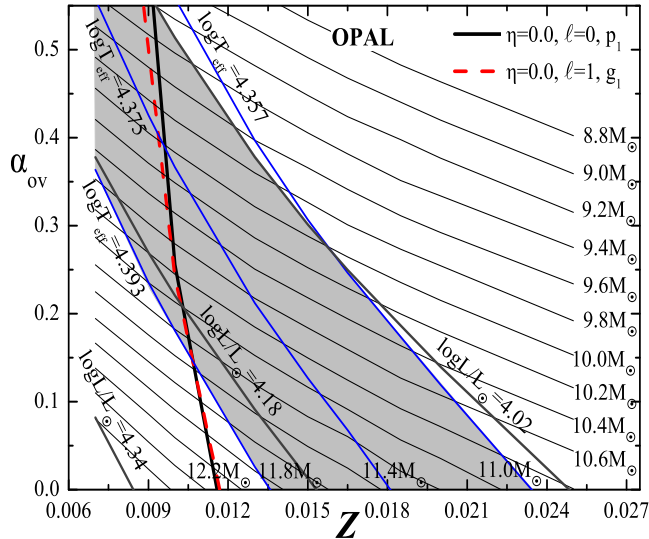


Figure 5. The overshooting parameter, α_{ov} , as a function of metallicity, Z , for seismic models of 12 Lac found from fitting the frequencies ν_4 and ν_2 (the modes $\ell = 0$, p_1 and $\ell = 1$, g_1 , respectively) for the hydrogen abundance of $X = 0.7$ and the OPAL opacities. There are plotted also lines of constant mass (thin, black), effective temperature (black), luminosity (grey) and instability borders for the radial p_1 mode (thick, solid) and dipole g_1 mode (thick, dotted). Models to the right of these lines are unstable. The grey area indicates models inside the error box.

these two values of V_{rot} . The ν_1 dipole mode was identified as the prograde mode ($m = 1$) and it is the second component of the g_1 triplet. The ν_3 quadruple mode is the prograde mode ($m = 1$) and it is a component of the g_1 quintuplet. For the ν_5 quadruple mode, Desmet et al. (2009) were able to derive only that $m \geq 0$ what for most models fit to the g_2 quintuplet.

As we have shown in Section 3, ν_A is the dipole retrograde mode ($\ell = 1$, $m = -1$). Identification of the radial order n for low frequency modes is very sensitive to the adopted value of the rotational velocity. Assuming $V_{rot} = 50$ km/s we got that ν_A is a g_{15} or g_{16} mode and for $V_{rot} = 80$ km/s - g_{13} or g_{14} are allowed.

The remaining frequencies of 12 Lac do not have unambiguous identifications of the angular numbers so their radial orders cannot be determined as well.

4 COMPLEX ASTEROSEISMOLOGY

Our seismic modeling can be divided into two parts. First, we computed pulsational models which fit two well identified axisymmetric pulsational frequencies. In the case of 12 Lac, these are ν_4 and ν_2 , identified as the radial fundamental and dipole g_1 modes, respectively. Then, the theoretical values of the complex nonadiabatic parameter f corresponding to these two frequencies were compared with the empirical counterparts. We termed this approach *complex seismic model*. Here, we construct complex seismic models for two sets of the opacity data (OPAL and OP), two sets of the model atmospheres (LTE and non-LTE), and two sets of

the chemical mixture (AGSS09 and the one derived for 12 Lac by Morel et al. (2006)).

4.1 Fitting frequencies

Fitting two, well-identified frequencies, ν_4 and ν_2 , for an assumed hydrogen abundance, $X = 0.7$, allow to relate the mass, M , and the overshooting parameter, α_{ov} , of seismic models with their metallicity, Z . These relations are presented in Fig. 5, where the overshooting parameter is plotted versus metallicity. Models with constant masses are marked with black, thin lines. Thick, solid line indicates instability border for the radial fundamental mode, while thick, dotted line - for the dipole g_1 mode. The instability borders of these two modes almost overlap and cover a very narrow range of metallicity, i.e., $Z \in (0.0105 - 0.0115)$. Models to the right of these lines are unstable. We marked also the lines of constant effective temperature and luminosity. The showed values of $\log T_{eff}$ and $\log L/L_{\odot}$ correspond to the center and edges of the observational error box.

As we can see, there are a lot of seismic models of 12 Lac fitting two frequencies, ν_4 and ν_2 . An accuracy of this fitting amounts to 10^{-6} c/d. In general, models with a given value of the core overshooting have smaller masses, if they have larger metallicity. On the other hand, models with constant mass have increasing metallicity with decreasing overshooting. These results are similar to those obtained for γ Peg (Walczak & Daszyńska-Daszkiewicz 2010, Walczak et al. 2013). The number of these seismic models can be limited if we take into account only unstable models and inside the observational error box (grey area). This slightly narrow the metallicity parameter, Z , which should be from about 0.010 up to 0.024. Unfortunately, we are not able to constrain the overshooting parameter, α_{ov} . There are seismic models with no overshooting from the convective core as well as with $\alpha_{ov} \sim 0.5$.

In the next step, we will check whether these models reproduce other well identified frequencies, i.e., $\nu_3 = 5.490167$ c/d - a quadruple prograde mode ($\ell = 2$, $m = 1$), $\nu_5 = 4.24062$ c/d - a quadruple prograde mode ($\ell = 2$, $m > 0$), and $\nu_A = 0.35529$ c/d - the dipole retrograde mode ($\ell = 1$, $m = -1$). The centroid values of these frequencies were calculated according to Eq. (12) for two values of the rotational velocity, 50 and 80 km/s. Lines of models fitting additionally one of these three frequencies are applied in Fig. 6. The left and right panels include models computed with the rotational splitting for $V_{rot} = 50$ and 80 km/s, respectively. The accuracy of the fitting of these three frequencies ranges from 10^{-5} to $5 \cdot 10^{-4}$ c/d.

As we can see, models computed with $V_{rot} = 50$ km/s reproduce ν_3 , ν_5 and ν_A as a g_{16} mode, only for high values of the overshooting parameter and quite high metallicities. Models fitting ν_A as a g_{15} mode are nearly on the horizontal line and give constraints on overshooting: $\alpha_{ov} \in (0.15, 0.31)$. Here, ν_5 can be only the quadruple sectoral mode ($\ell = 2$, $m = +2$). In the case of models computed with $V_{rot} = 80$ km/s, we obtained lower values of the overshooting parameter. The frequency ν_A has now lower radial order: $n = 13$ for $\alpha_{ov} \in (0.05, 0.24)$ and $n = 14$ for $\alpha_{ov} \in (0.4, 0.5)$. The frequency ν_5 can be either $m = +2$ for $\alpha_{ov} \in (0.1, 0.38)$ or $m = +1$ for $\alpha_{ov} \approx 0.5$ and $Z > 0.018$.

It is worth to notice that models fitting additionally

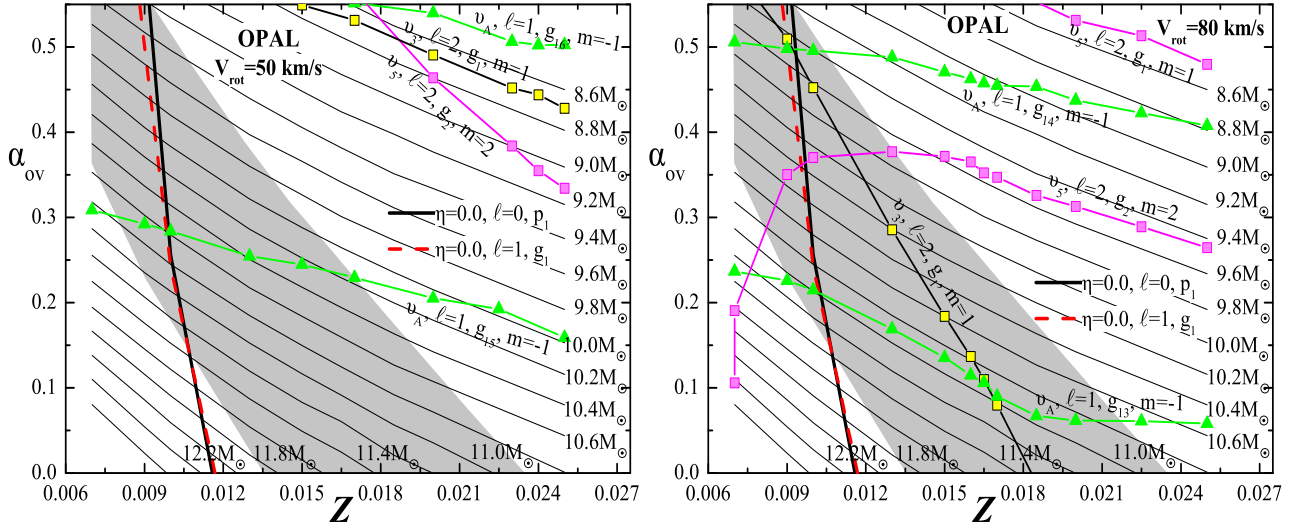


Figure 6. The same as in Fig. 5 but we added lines of models fitting the third frequency: ν_3 or ν_5 or ν_A . The left and right panels correspond to models computed with the rotational splitting for $V_{\text{rot}} = 50$ and 80 km/s, respectively. The grey area indicates the observational error box.

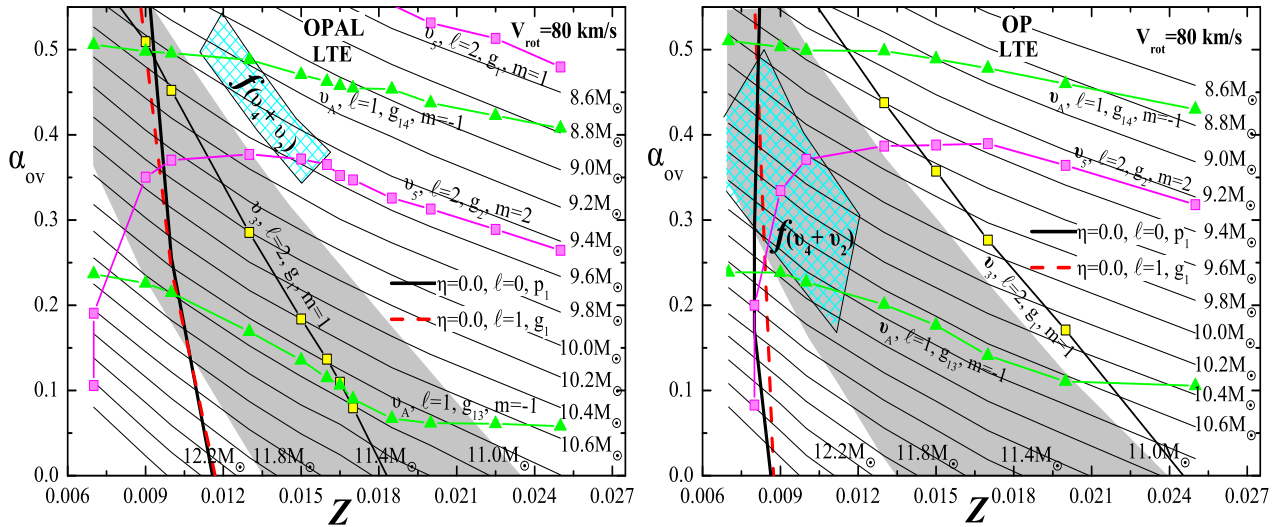


Figure 7. The same as in the right panel of Fig. 6, but we marked models fitting the empirical values of the nonadiabatic f -parameter (hatched areas) of both the radial fundamental mode and dipole g_1 mode (labeled as $f(\nu_4 + \nu_2)$). In the left panel, we used the OPAL data and in the right panel the OP opacities. In both cases we assumed the AGSS09 mixture and the rotational splitting for $V_{\text{rot}} = 80$ km/s. The LTE model atmospheres with the microturbulent velocity of $\xi_t = 2$ km/s were used.

the frequency ν_A are usually on the nearly horizontal lines, i.e., they have nearly constant overshooting regardless of the metallicity. Thus, the high-order g-modes could be potentially good indicators of α_{ov} but proper identification of n is crucial. A similar behaviour can be seen in the case of models fitting additionally ν_5 except for the small values of metallicity, $Z < 0.01$. On the other hand the line of models fitting additionally the frequency ν_3 corresponding to $(\ell = 2, m = +1, g_1)$, has the largest slope, i.e., the largest dependence of α_{ov} on Z . In general, models fitting pressure modes form the sloped lines on the the α_{ov} vs. Z plane whereas models fitting gravity and mixed modes - nearly horizontal lines.

As we can see from the right panel of Fig. 6, there are a few intersections of two lines which means that we have models fitting four frequencies simultaneously: $(\nu_4, \nu_2, \nu_3, \nu_A)$ or $(\nu_4, \nu_2, \nu_5, \nu_A)$ or $(\nu_4, \nu_2, \nu_3, \nu_5)$.

4.2 Fitting the f -parameters

Each pulsational frequency is associated with the non-adiabatic complex parameter f which gives the ratio of the bolometric flux changes to the radial displacement. This quantity is very sensitive to properties of subphotospheric layers where mode driving occurs. In the case of B-type pulsators, f shows a strong dependence on metallicity and

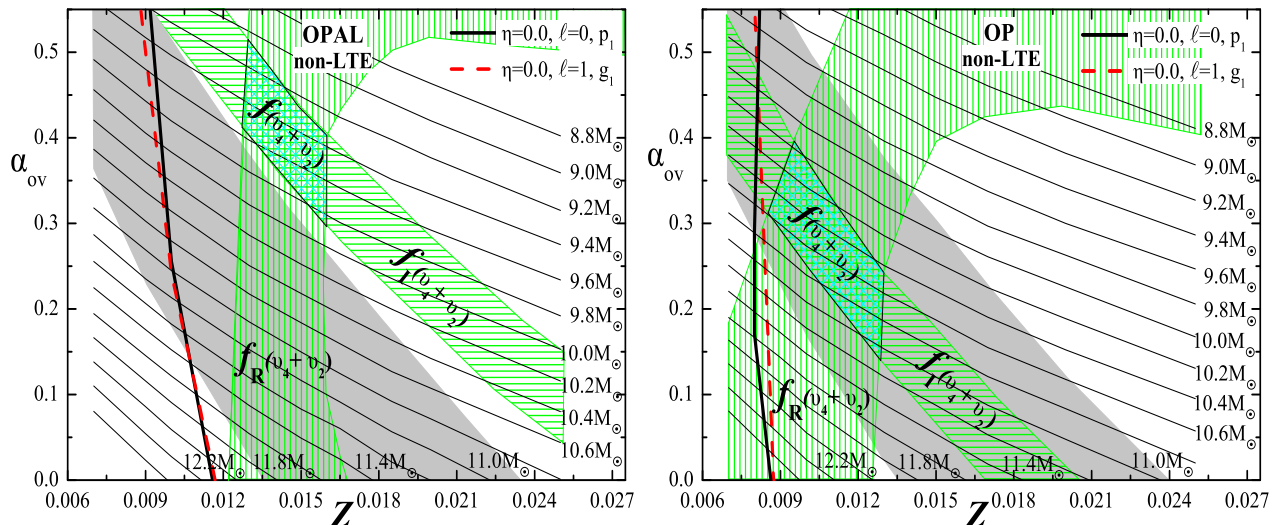


Figure 8. The same as in Fig. 7, but we used the non-LTE model atmospheres in order to derive the empirical values of the f -parameter. There are also shown models which fit separately the real (vertical bars) and imaginary (horizontal bars) parts of f .

opacity data. Thus, a comparison of the theoretical and empirical values of f may yield constraints on these quantities (Daszyńska-Daszkiewicz, Dziembowski & Pamyatnykh, 2005).

In a set of seismic models fitting the frequencies ν_4 and ν_2 , we tried to find those which reproduce also both values of the f -parameter within the observational errors. Such models exist and are marked as hatched areas in Fig. 7 on the Z vs. α_{ov} planes and are labeled as $f(\nu_4 + \nu_2)$. The left and right panels correspond to models computed with the OPAL and OP data, respectively. To derive the empirical values of f , we used the LTE model atmospheres with the microturbulent velocity of $\xi_t = 2$ km/s (Kurucz 2004).

As we can see, the hatched regions are quite small, what substantially reduces the number of models. The OPAL seismic models are slightly outside the observational error box of 12 Lac. They are cooler and less luminous. They have also a high overshooting parameter, $\alpha_{ov} \sim 0.35 - 0.55$. The OP seismic models have smaller metallicity and overshooting. In this case, the area $f(\nu_4 + \nu_2)$ is larger and entirely inside the error box, suggesting a preference for the OP tables. In the case of the high-order g-mode, ν_A , all OPAL models fitting this frequency reproduce also the empirical values of f . The line ($\ell = 1, g_{14}$) crosses the area $f(\nu_4 + \nu_2)$ for $\alpha_{ov} \approx 0.5$ and $Z \approx 0.014$. Also almost all OP models fitting the frequency ν_A reproduce its value of f ; except for models with the core overshooting of $\alpha_{ov} \approx 0.45$ and metallicity of $Z \approx 0.020 - 0.025$. In this case the line ($\ell = 1, g_{13}$) crosses the area $f(\nu_4 + \nu_2)$ for $\alpha_{ov} \approx 0.2$ and $Z \approx 0.011$. Thus with both opacity OP tables, we get seismic models reproducing the three frequencies ν_4 , ν_2 , ν_A and their f -parameters simultaneously, but only the OP models are located inside the observational error box and have „reasonable” values of the core overshooting. In the case of ν_3 and ν_5 , no seismic model reproduces their values of f in the allowed range of parameters, neither with the OPAL and OP data.

Comparing the OPAL and OP seismic models, we can conclude that for a given Z and α_{ov} , models calculated with these two opacity tables have similar masses, effective tem-

peratures and luminosities. Instability borders for the radial fundamental and dipole g_1 modes are slightly larger for the OP tables. The positions of lines representing models fitting additionally ν_5 or ν_A are quite similar, the difference is that in the case of the OP models, there is no mode $\ell = 2, m = +1, g_2$ for ν_5 . The biggest change is connected with ν_3 . The line of the OP models fitting the frequency ν_3 is shifted toward much larger metallicities.

The empirical values of the f -parameter depend slightly on the model atmospheres, so we decided to check this effect. In Fig. 8, we show models fitting the empirical values of f for the ν_4 and ν_2 frequencies derived with the non-LTE models of stellar atmospheres (Lanz & Hubeny, 2007). In the left and right panels we used the OPAL and OP opacity tables, respectively. Additionally, we marked models fitting separately the real, f_R , (vertical bars) and imaginary, f_I , (horizontal bars) parts of the f -parameter. As we can see, the overshooting parameter of models fitting f_I decreases with increasing metallicity. In the case of models fitting the real part of f , the dependence of α_{ov} on Z is different. First, for low values of Z , the overshooting parameter increases rapidly with metallicity and then, for larger Z , it starts to decrease. With the LTE atmospheres, the shape of the regions fitting the real and imaginary part of f is similar; the main difference is in positions of the regions. The theoretical values of f for ν_4 and ν_2 fit the empirical counterparts derived with the non-LTE atmospheres for slightly larger metallicity and lower core overshooting.

4.3 Effects of the chemical mixture and the opacity enhancement

To evaluate the effect of the adopted chemical mixture, we performed our seismic modeling assuming the photospheric chemical element abundances of 12 Lac as derived by Morel et al. (2006). In Fig. 9, we show the results on the α_{ov} vs. Z plane. The left and right panels correspond to computations with the OPAL and OP data, respectively. In

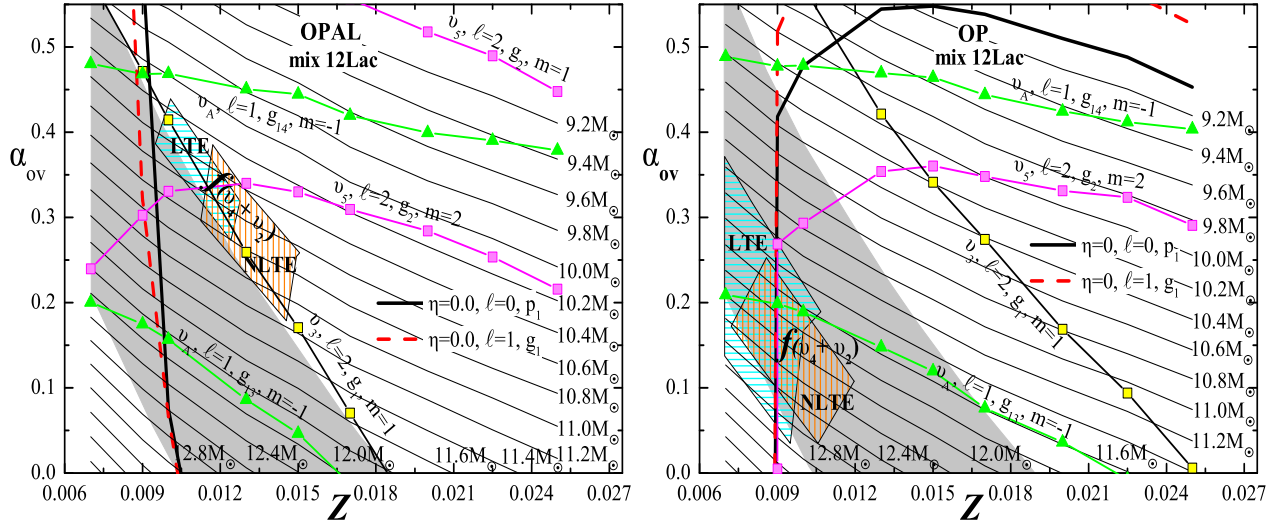


Figure 9. The same as in Fig. 5 but for models computed for the 12 Lac mixture. We marked models reproducing the empirical values of the nonadiabatic f -parameter of both ν_4 and ν_2 , obtained with the LTE (horizontal bars) and non-LTE (vertical bars) atmospheres. In the left panel we used the OPAL data and in the right panel the OP tables.

both cases, the empirical values of f were determined adopting both the LTE (horizontal bars) and non-LTE (vertical bars) model atmospheres.

In a comparison with computations performed with AGSS09 and $X = 0.7$, now the models fitting additionally the f -parameters of ν_4 and ν_2 have considerably lower values of the core overshooting parameter, while their metallicity parameter was not changed much. The mean value of α_{ov} for models fitting the f -parameters with the 12 Lac mixture is approximately 0.13 lower. The lower overshooting occurs for both OP and OPAL opacities as well as for the LTE and non-LTE atmospheres. The lines of constant masses and a position of a grey area corresponding to the error box were also moved towards lower overshooting. These changes are caused mainly by a higher hydrogen abundance, $X = 0.764$, which we adopted after Morel et al. (2006). Abundances of others elements had no significant influence on the results. As we can see lines of models fitting additionally one of the three frequencies ν_3 , ν_5 , ν_A , also follow the general trend, i.e., a shift towards slightly lower values of α_{ov} . In the case of the OPAL data, models fitting the f -parameters are still mostly outside the error box. Amongst seismic models computed with the OP tables, there are those that fit also the frequency ν_A and its values of the f -parameter. Thus, also with the 12 Lac mixture, there exist seismic models fitting these three frequencies and corresponding values of the f -parameter simultaneously.

To summarize, we constructed seismic models with two sets of opacity tables, two sets of model atmospheres, two values of microturbulent velocity and two mixtures of chemical elements. Now, the question is which case is „the best”. To pre-answer this question, in Table 2, we listed the models with the minimum values of χ^2 for each case. These models reproduce the centroid frequencies, ν_2 and ν_4 , and their empirical values of the f -parameter. The values of χ^2 were obtained from fitting the photometric and radial velocity amplitudes and phases when de-

termining the empirical values of f for ν_2 and ν_4 (see Sect. 3.1 for the description of the method).

In the next step, we were trying to find a model fitting the first five frequencies, ν_1 , ν_2 , ν_4 , ν_3 , ν_5 , as well as ν_A . We did it by setting the value of the rotational velocity which gives an adequate splitting for ν_1 , ν_3 , ν_5 , ν_A . We obtained $V_{rot} = 74.6$ km/s what is consistent with the value suggested by Dziembowski & Pamyatnykh (2008) for the inner part of the star. In the case of these four mode a significant contribution to the kinetic energy density comes from the g-mode propagating zone and their splitting is mainly determined by the inner layers which presumably rotate faster. This rotational rate agrees also with the value of V_{rot} obtained from identification of the angular numbers of the g-mode frequency, ν_A , (cf. the right panel of Fig. 3). In Fig. 10, we compare the observed frequency spectrum of 12 Lac with the theoretical one corresponding to the model reproducing the six frequencies. The model has the following parameters: $M = 10.28M_\odot$, $\log T_{eff} = 4.347$ and $\log L/L_\odot = 4.00$, and was computed for the metallicity $Z = 0.0115$, overshooting parameter $\alpha_{ov} = 0.39$, OPAL tables and the 12 Lac mixture. We called it MODEL-6 ν and it is marked as an asterisk in the HR diagram (Fig. 1). The theoretical p-modes were split according to the rotational rate of $V_{rot} = 50$ km/s which corresponds to the outer layers.

As we can see in Fig. 10, the dipole prograde mode reproduces very well the dominant frequency, ν_1 . The frequency ν_6 , identified as $\ell = 1$ or 2 is quite close to the centroid of $\ell = 1$, p_2 and to $\ell = 3$, p_0 with $m = +2, +3$. The frequency ν_9 could be $\ell = 3, m = -3$, p_0 or $\ell = 2, m = 0$, p_0 but $\ell = 2$ was excluded in our identification for this frequency. The value of ν_7 is not far from $\ell = 2, m = 0$, g_1 and for ν_8 , identified as $\ell = 2$, the closest counterpart is $\ell = 3, m = +1$, g_2 . The frequency ν_{10} , identified as $\ell = 1$ or 2, is very close to $\ell = 1, m = +1$, p_1 .

In Table 3, we compare the theoretical values of the f -parameter for MODEL-6 ν with the empirical counterparts derived with the LTE model atmospheres. The first and sec-

Table 2. A list of the „best” seismic models for each considered case. The basic stellar parameters are given in columns 2 – 6. The last two columns contains the values of χ^2 as determined from fitting the photometric and radial velocity amplitudes and phases for ν_2 and ν_4 , respectively.

Model	Z	α_{ov}	$M [M_{\odot}]$	$\log T_{\text{eff}}$	$\log L/L_{\odot}$	$\chi^2(\nu_2)$	$\chi^2(\nu_4)$
OPAL LTE $\xi_t = 8$	0.0135	0.45	9.3027	4.3463	3.9711	2.00	2.76
OPAL LTE $\xi_t = 2$	0.0135	0.40	9.5440	4.3513	3.9973	3.54	4.05
OPAL NLTE $\xi_t = 2$	0.0160	0.30	9.8440	4.3501	4.0003	2.77	3.45
OPAL mix12Lac LTE	0.0100	0.41	10.289	4.3522	4.0217	3.49	3.84
OPAL mix12Lac NLTE	0.0125	0.25	10.922	4.3549	4.0469	4.54	6.58
OP LTE $\xi_t = 2$	0.0115	0.32	10.152	4.3693	4.0846	8.95	5.80
OP NLTE $\xi_t = 2$	0.0130	0.24	10.462	4.3704	4.0962	6.20	5.32
OP mix12Lac LTE	0.0100	0.21	11.494	4.3733	4.1322	10.98	6.46
OP mix12Lac NLTE	0.0115	0.12	11.899	4.3749	4.1464	7.62	5.11

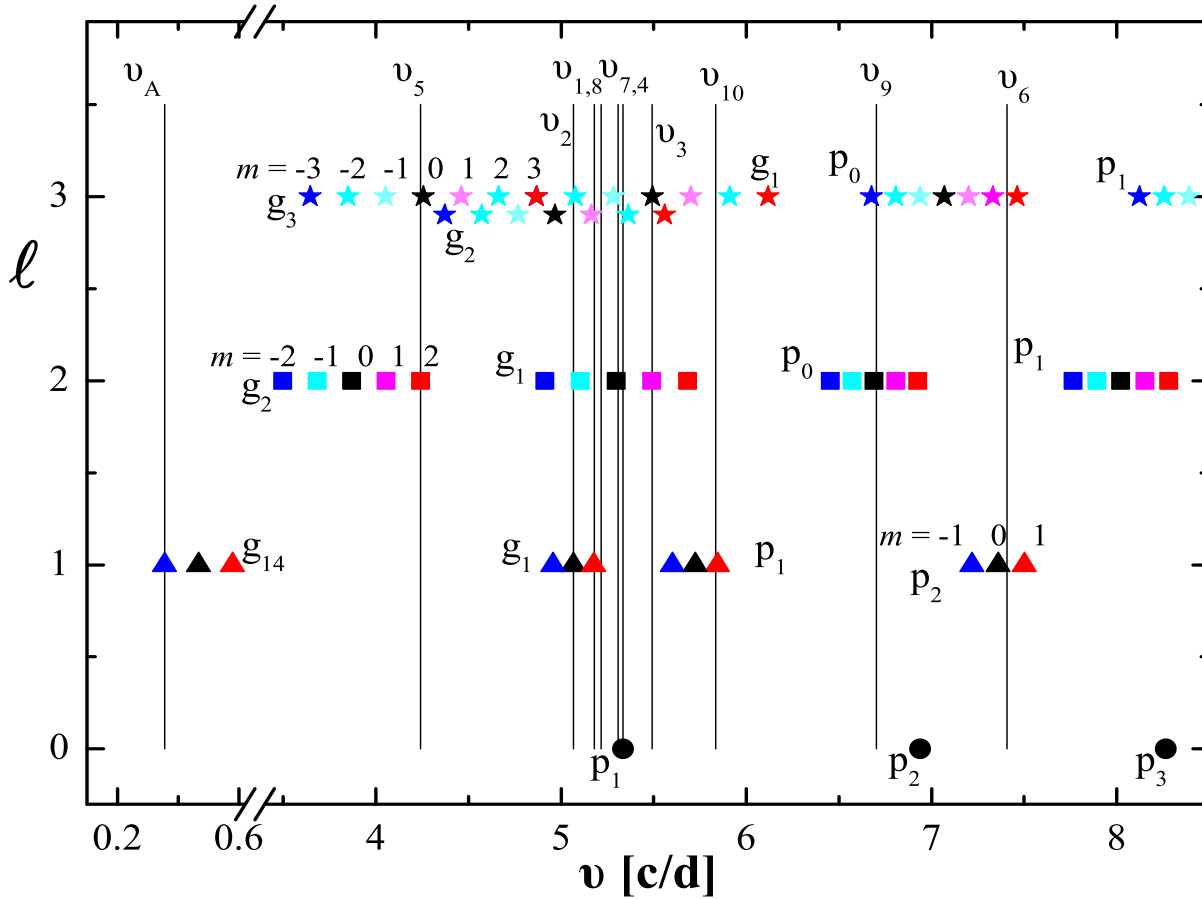


Figure 10. Comparison of the observed frequencies of 12 Lac (vertical lines) with theoretical ones (symbols) corresponding to MODEL- 6ν fitting six frequencies: ν_1 , ν_2 , ν_3 , ν_4 , ν_5 and ν_A . The value of the rotational splitting was computed at $V_{\text{rot}} = 50$ km/s for p-mode frequencies and at $V_{\text{rot}} = 74.6$ km/s for g-mode frequencies. The mode degrees $\ell = 0, 1, 2, 3$ were considered.

and lines for each frequency correspond to the empirical and theoretical values, respectively. There is no ν_7 because it was not found in the radial velocity variations. For the frequencies ν_6 , ν_9 and ν_{10} , we gave the two values of f obtained for mode degrees, ℓ , as listed in Table 1. The differences in f resulting from adopting different model atmospheres are small; the f -parameter derived with the non-LTE atmospheres is

usually slightly lower. In the first column of Table 3, we list the empirical values of the intrinsic mode amplitude, ε , multiplied by the spherical harmonic, $|\tilde{\varepsilon}| = |\varepsilon Y_{\ell}^m(i, 0)|$, where i is the inclination angle.

For the radial mode, ν_4 , the value of $|\tilde{\varepsilon}|$ is equal to $|\varepsilon|$, i.e., to the root mean square of the relative change of the stellar radius, $\delta r/R$, over the surface. Because we have

Table 3. The empirical values of $|\varepsilon| = |\varepsilon|Y_\ell^m(i, 0)$, the empirical and theoretical values of the f -parameter, the instability, η , and the value of χ_E^2 for all detected frequencies of 12 Lac. We used the stellar model fitting six frequencies: $\nu_1, \nu_2, \nu_3, \nu_4, \nu_5$ and ν_A (MODEL-6 ν). The empirical values of f were derived with the LTE model atmospheres.

mode		$ \varepsilon $	f_R	f_I	η
$\nu_{1,\ell=1}$	empir	0.01431(62)	-8.41(37)	-1.24(38)	—
	teor	—	-7.97	-0.11	0.05
$\nu_{2,\ell=1}$	empir	0.00660(37)	-7.69(44)	-0.20(44)	—
	teor	—	-7.77	-0.23	0.053
$\nu_{3,\ell=2}$	empir	0.00429(41)	-10.7(1.3)	-0.6(1.3)	—
	teor	—	-8.62	0.23	0.041
$\nu_{4,\ell=0}$	empir	0.00631(22)	-8.23(33)	-0.31(33)	—
	teor	—	-8.17	0.06	0.044
$\nu_{5,\ell=2}$	empir	0.00187(14)	-4.53(75)	-4.96(75)	—
	teor	—	-6.52	-0.90	0.087
$\nu_{6,\ell=1}$	empir	0.00029(6)	-20.6(4.0)	4.4(4.0)	—
	teor	—	-11.59	3.21	-0.148
$\nu_{6,\ell=2}$	empir	0.00046(6)	-23.5(3.1)	4.2(3.1)	—
	teor	—	-11.71	3.21	-0.153
$\nu_{8,\ell=2}$	empir	0.00163(30)	5.1(1.9)	4.7(1.9)	—
	teor	—	-8.17	-0.07	0.052
$\nu_{9,\ell=1}$	empir	0.00070(12)	-6.0(1.3)	3.3(1.3)	—
	teor	—	-10.53	1.96	-0.056
$\nu_{9,\ell=3}$	empir	0.00300(15)	-13.3(1.8)	23.2(1.8)	—
	teor	—	-10.78	1.91	-0.059
$\nu_{10,\ell=1}$	empir	0.00056(10)	-7.2(1.3)	-0.9(1.4)	—
	teor	—	-9.11	0.68	0.02
$\nu_{10,\ell=2}$	empir	0.00074(17)	-4.4(2.2)	-3.0(2.2)	—
	teor	—	-9.20	0.66	0.023
$\nu_A, \ell=1$	empir	0.00053(25)	26.3(12.5)	-2.9(12.0)	—
	teor	—	18.13	5.37	-0.631

identification of the mode degree, ℓ , and azimuthal order, m , for $\nu_1, \nu_2, \nu_3, \nu_5$ and ν_A as well as the inclination angle, $i \approx 48^\circ$, (Desmet et al. 2009), we were able to derive the relative change of the stellar radius also for these modes. As a result we obtained that $|\varepsilon|$ is equal to: 1.57% for ν_1 , 0.57% for ν_2 , 0.32% for ν_3 , 0.63% for ν_4 , 0.25% for ν_5 (assuming that $\ell = 2, m = 2$) and 0.06% for ν_A . The amplitude of the relative radius changes caused by radial pulsations of 12 Lac is similar to that of other β Cep stars. For example, $|\varepsilon|$ of the radial mode for θ Oph is equal to 0.14% (Daszyńska-Daszkiewicz & Walczak 2009), for ν Eri - 1.72% (Daszyńska-Daszkiewicz & Walczak 2010) and for γ Peg - 0.26% (Walczak & Daszyńska-Daszkiewicz 2010). The last column contains the value of the instability parameter η . Some of these modes are stable ($\eta < 0$). The most negative value is for the high-order g-mode, ν_A , and amounts to -0.63 , what asserts the well-known problem of excitation of high-order g-modes in the massive main sequence pulsators.

The last issue we would like to examine is the effect of the opacity enhancement. The reason is that for 12 Lac, as well as for some other β Cephei stars, there was pos-

tulated an increase of stellar opacities near the Z-bump (Pamyatnykh, Handler & Dziembowski 2004; Miglio et al. 2007; Dziembowski & Pamyatnykh 2008). This should have solved the problem with instability of some modes as well as improve fitting frequencies. We decided to test the artificial opacity enhancement near this opacity bump. To this aim, we increased the opacity coefficient in the OPAL tables by 50% in the metal bump. The obtained seismic models fitting two frequencies, ν_4 and ν_2 , were not changed much. The masses, effective temperatures and luminosities were similar. As one could expect, the biggest difference is related to the instability. With higher opacities, all our models have unstable modes $\ell = 0, p_1$ and $\ell = 1, g_1$, even for $Z = 0.007$. It turned out, that models calculated with the modified OPAL table mimic those computed with the original OP data. It is connected with the internal differences between the two opacity tables; the OP data provide larger opacity coefficient near the Z-bump.

However, with the modified opacities we did not manage to find models fitting the empirical values of the f -parameter, neither for ν_4 nor for ν_2 . The increase of the opacity coefficient changed significantly the real part f whereas the imaginary part of f was almost insensitive to the opacity increase. Although the increase of the opacity parameter can solve problems with instabilities, a disagreement between the empirical and theoretical values of f argues against this change. The same result was obtained for γ Pegasi (Walczak & Daszyńska-Daszkiewicz 2010, Walczak et al. 2013).

5 CONCLUSIONS

The aim of the paper was to construct complex seismic models of the β Cep/SPB star 12 Lacertae, i.e., models which fit simultaneously pulsational frequencies and the corresponding values of the nonadiabatic parameter f . As usually, we began with the mode identification from the multi-colour photometry and radial velocity data. Unambiguous determination of ℓ was possible for the six frequencies of 12 Lac; for the remaining ones usually two possibilities were obtained. Moreover, for the dominant mode, ν_1 , and the high-order g-mode, ν_A , the effects of rotation on identification of ℓ were checked. As a result we got that ν_1 is the pure (non-rotational coupled) dipole mode and ν_A is the dipole retrograde mode.

We found plenty of models which reproduce the two centroid frequencies ν_4 and ν_2 , identified as $\ell = 0, p_1$ and $\ell = 1, g_1$, respectively, and their empirical values of the f -parameter simultaneously. These models are inside the observational error box only if the OP opacity tables were used. Models computed with the OPAL data had too small effective temperatures and luminosities. The next argument for the OP tables is that with this data, there exist models which fit additionally the high-order g-mode frequency, ν_A , identified as $\ell = 1, m = -1, g_{13}$, and its values of f for quite low values of the core overshooting, $\alpha_{ov} \approx 0.2$. With the OPAL data such models exist only for $\alpha_{ov} \approx 0.5$. Thus, we managed to find models which reproduce the three frequencies and their f -parameters simultaneously. This is the first star for which such a good concordance was achieved. Moreover, we showed that if one assumes the rotational velocity of the order of 75 km/s for the rotational splitting of

the gravity and mixed modes, then there exist models fitting the four frequencies and a model which fits the six frequencies (the first five and the low frequency ν_A). This value of the rotational velocity agrees with the result obtained from identification of ℓ and m for the high-order g-mode frequency ν_A . It confirms also the rotational rate suggested by Dziembowski & Pamyatnykh (2008) for the interior of 12 Lac.

Similarly to the case of the hybrid pulsator γ Pegasi, we got that an increase of opacities in the metal bump spoils an agreement between the empirical and theoretical values of the non-adiabatic parameter f . Thus, our conclusion is the same: if modifications of the opacity tables are needed they have to be done in a more detailed way.

ACKNOWLEDGMENTS

We thank Gelard Handler for providing us with data on the light variations in the *uvy* passbands and Maarten Desmet for data on the radial velocity variations. This work was partially supported by the Human Capital Programme grant financed by the European Social Fund.

REFERENCES

- Adams W.S., 1912, ApJ, 35, 163
 Asplund M., Grevesse N., Sauval A.J., Scott P., 2009, ARA&A, 47, 481
 Baglin A., Michel E., Auvergne M., The COROT Team 2006, in Proc. SOHO 18/GONG 2006/HELAS I, Beyond the spherical Sun, ESA SP, Sheffield, 624
 Barning F. J. M., 1963, Bull. Astr. Inst. Netherlands, 17, 22
 Christie W. H., 1926, Pop. Astr., 34, 551
 Ciurla T., 1987, AcA, 37, 53
 Claret A., 2000, A&A, 363, 1081
 Daszyńska-Daszkiewicz J., Dziembowski W. A., Pamyatnykh A. A., Goupil, M.-J., 2002, A&A, 392, 151
 Daszyńska-Daszkiewicz J., Dziembowski W. A., Pamyatnykh A. A., 2003, A&A, 407, 999
 Daszyńska-Daszkiewicz J., Dziembowski W. A., Pamyatnykh A. A., 2005, A&A, 441, 641
 Daszyńska-Daszkiewicz J., Szewczuk W., 2011, ApJ, 728, 17
 Daszyńska-Daszkiewicz J., Walczak P., 2009, MNRAS, 398, 1961
 Daszyńska-Daszkiewicz J., Walczak P., 2010, MNRAS, 403, 496
 de Jager C., 1953, BAN, 12, 81
 de Jager C., 1963, Bull. Astr. Inst. Netherlands, 17, 1
 Desmet M., Briquet M., Thoul A., Zima W., De Cat P., Handler G., Ilyin I., Kambe E., Krzesinski J., Lehmann H., Masuda S., Mathias P., Mkrtichian D. E., Telting J., Uytterhoeven K., Yang S.L.S., Aerts C., 2009, MNRAS, 396, 1460
 Dziembowski W. A., 1977, AcA, 27, 203
 Dziembowski W. A., Jerzykiewicz M., 1999, A&A, 341, 480
 Dziembowski W. A., Pamyatnykh A. A., 2008, MNRAS, 385, 2061
 Fath E. A., 1938, Pop. Astr., 46, 241
 Fath E. A., 1947, AJ, 52, 123
 Ferguson, J. W., Alexander, D.R., Allard, F., 2005, ApJ, 623, 585
 Grevesse N., Noels A., 1993, in Pratzko N., Vangioni-Flam E., Casse M., eds, Origin and Evolution of the Elements. Cambridge Univ. Press, Cambridge, p. 15
 Guthnick P., 1919, AN, 208,219
 Handler, G., Jerzykiewicz, M., Rodríguez, E., at al., 2006 MNRAS, 365, 327
 Iglesias C. A., Rogers F. J., 1996, ApJ, 464, 943
 Jarzebowski T., Jerzykiewicz M., Musielok B., Le Contel J.-M., 1979, AcA, 29, 517
 Jerzykiewicz M., 1978, AcA, 28, 465
 Jerzykiewicz M., Musielok B., Borkowski K. J., 1984, AcA, 34, 21
 Koch D. G., Borucki W. J., Basri G.: 2010, ApJ 713, 79
 Kurucz R. L., 2004, <http://kurucz.harvard.edu>
 Lanz T., Hubeny I., 2007, ApJS, 169, 83
 Lee, U. & Saio, H., 1997, ApJ., 491, 839
 Mathias P., Aerts C., Gillet D., Waelkens C., 1994, A&A, 289, 875
 Miglio, A., Bourge, P.-O., Montalbán, J., Dupret, M.-A., 2007, CoAst, 150, 209
 Morel T., Butler K., Aerts C., Neiner C., Briquet M., 2006, A&A, 457, 651
 Pamyatnykh A. A., Dziembowski W. A., Handler G., Pikall H., 1998, A&A, 333, 141
 Pamyatnykh A. A., Handler G., Dziembowski W. A., 2004, MNRAS, 350, 1022
 Rogers F. J., Nayfonov A., 2002, ApJ, 576, 1064
 Sato N., 1979, Ap&SS, 66, 309
 Seaton M. J., 2005, MNRAS, 362, 1
 Serenelli A. M., Basu S., Ferguson J. W., Asplund, M., 2009, ApJ, 705, 123
 Smith M. A., 1980, ApJ, 240, 149
 Soufi, F., Goupil, M.-J., Dziembowski, W. A., 1998, A&A, 334, 911
 Stebbins J., 1917, Pop. Astr., 25, 657
 Townsend, R.H.D. 2003, MNRAS, 340, 1020.
 Young R. K., 1915, Publ. Dom. Obs. Ottawa, 3, 63
 Young R. K., 1919, JRASC, 13, 45
 Walczak P. & Daszyńska-Daszkiewicz J., 2010, AN, 331, 1057
 Walczak P., Daszyńska-Daszkiewicz J., Pamyatnykh A. A., Zdravkov T., 2013, in preparation
 Walker G., Matthews J., Kuschnig R. at al.: 2003, PASP 115, 1023